# Pseudoazurin–Nitrite Reductase Interactions

Antonietta Impagliazzo,[a] Ludwig Krippahl,[b] and Marcellus Ubbink*[a]

*The nitrite reductase-binding site on pseudoazurin has been determined by using NMR chemical-shift perturbations. It comprises residues in the hydrophobic patch surrounding the exposed copper ligand His81 as well as several positively charged residues. The binding site is similar for both redox states of pseudoazurin, despite differences in the binding mode. The results suggest that pseudoazurin binds in a well-defined orientation. Docking simulations provide a putative structure of the complex with a binding site on nitrite reductase that has several hydrophobic and polar residues as well as a ridge of negatively charged side chains and a copper-to-copper distance of 14 Å.*

## Introduction

In many cellular redox reactions, electrons are donated by general electron carriers, like the NADPH cofactor or small electron-transfer (ET) proteins. In the latter case, the ET protein must associate transiently with the redox enzyme to allow ET through the enzyme towards the substrate. Association and dissociation of the ET protein must be fast in order not to limit the turnover of the redox enzyme. These requirements can be met by a strong electrostatic attraction between the ET protein and the enzyme, to enhance the association rate constant, combined with moderate surface matching of the binding interface, to ensure rapid dissociation.[1,2]

Nitrite reductase (NiR) from the soil bacterium *Alcaligenes faecalis* S-6 catalyses the reduction of nitrite to nitric oxide. This is one of the reactions of denitrification, which is an important process in the global nitrogen cycle. NiR is a 110 kDa homotrimeric protein that contains six copper ions (Figure 1). Three coppers ions, in type 2 copper sites,[3] are part of the three active sites located on the interface of the subunits while the remaining copper ions are buried within the subunits, forming type 1 copper sites. Electrons are donated by a small ET protein, pseudoazurin (PAZ),[4] and transferred to the active site by the type 1 copper ions. PAZ is a 14 kDa protein that also contains a type 1 copper centre.

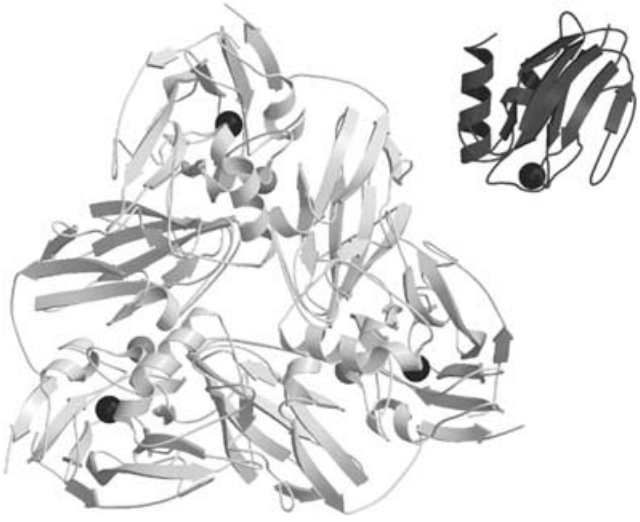

**Figure 1.** NiR and PAZ are shown in ribbon representations. NiR is in light grey and PAZ in dark grey. The spheres represent copper ions. The type 1 copper ion in NiR is shown in black, the type 2 copper ion in grey.

Both proteins are highly charged. In PAZ, eight lysine residues of a total of 13 and Arg114 form a positively charged ring around a hydrophobic patch through which the copper ligand His81 protrudes slightly. A molecular dipole is created by the presence of four negatively charged residues (Asp29, Asp47, Asp94 and Asp100) at the other end of the protein.[5] NiR is characterised by 40 negatively and 27 positively charged residues per monomer; this results in an overall negatively charged surface.[6]

Kinetic studies[7,8] on the interaction of NiR and PAZ have demonstrated that electrostatic attraction contributes to the binding affinity. Nine lysine residues on the PAZ surface were replaced one by one with alanine or aspartate. Variants of the residues Lys10, Lys38, Lys57 and Lys77 exhibited a decreased affinity for NiR, evidenced by an increase of the $K_m$. However, the rate of electron transfer to NiR was not affected strongly for any of the mutants. Similarly, mutagenesis of ten negatively charged residues on NiR revealed the importance of several charged residues for pseudoazurin binding.

Recently, we found evidence based on NMR-binding studies for a redox state-dependent difference in the binding mode of PAZ to NiR. The oxidised form of PAZ, PAZ $Cu^{II}$, binds in a single, transient mode, while the reduced form, PAZ $Cu^{I}$, exhibits two modes, one weak, transient mode and one more strongly with a low dissociation rate (ref. [9] and unpublished results). For the slow mode, the NiR-binding site on PAZ could be determined,[9] and it was shown that the ring of positive charges and the hydrophobic patch participate in binding.

[a] *Dr. A. Impagliazzo, Dr. M. Ubbink*
*Leiden Institute of Chemistry, Leiden University*
*P.O. Box 9502, 2300 RA Leiden (The Netherlands)*
*Fax: (+31) 71-527-4349*
*E-mail: m.ubbink@chem.leidenuniv.nl*

[b] *Dr. L. Krippahl*
*Departamento de Química, FCT, Universidade Nova de Lisboa*
*2825 Monte de Caparica (Portugal)*

  DOI: 10.1002/cbic.200500082 

Here, we report the NiR-binding sites on PAZ for the fast-binding modes of both PAZ redox states and for various redox states of NiR. On the basis of a docking simulation using the experimental data a model of the complex structure is proposed.

## Results

### The complex between PAZ $Cu^{I}$ and NiR $Cu^{I}$-T2D

In order to determine the binding site for NiR on PAZ $Cu^{I}$ in its fast, transient binding mode, $^{15}N$-labeled PAZ was titrated into a solution of NiR and its NMR signals were observed in $^{1}H,^{15}N$-HSQC experiments. To avoid reactions with traces of dioxygen, the type 2 copper ions had been removed from the NiR (NiR $Cu^{I}$-T2D). The slow binding mode results in a loss of signal intensity of the PAZ resonances. The remaining signals represent the fraction of free PAZ, which experiences a weak, fast binding mode, evidenced by chemical-shift changes due to the presence of NiR.

The average backbone-amide chemical-shift perturbations ($\Delta\delta_{Avg}$) for PAZ $Cu^{I}$ at a ratio NiR $Cu^{I}$-T2D/PAZ of 1.7 are plotted in Figure 2a. Figure 3a shows the location of the affected residues mapped onto the crystal structure of PAZ,[5] coloured as indicated in Figure 2a. The majority of the affected residues lie in a region close to the copper ligand His81, which comprises nonpolar, polar and positively charged side chains.

As a control, NiR $Cu^{I}$–$Cu^{I}$ was titrated into a solution of $^{15}N$-PAZ $Cu^{I}$ under rigorously anaerobic conditions, giving the same results.

### The complex between PAZ $Cu^{II}/Zn^{II}$ and NiR Cu–Cu

In order to identify the binding surface of the complex between PAZ in the oxidised form and NiR, the copper atom of PAZ was replaced by $Zn^{II}$. $Zn^{II}$ is redox inactive; this enabled the analysis of the interaction with both reduced and oxidised NiR without the interference of ET events. $Zn^{II}$ is also diamagnetic, contrary to $Cu^{II}$. The paramagnetic cupric state causes severe broadening of the proton resonances in the vicinity of the metal, hindering their detection in standard NMR experiments. A recently determined crystal structure showed no significant differences between PAZ Cu and PAZ Zn.[10]

Titration of NiR into either $^{15}N$-PAZ $Cu^{II}$ or $^{15}N$-PAZ $Zn^{II}$ results in severe broadening of all signals, accompanied by chemical-shift perturbations, best observed in PAZ $Zn^{II}$. This indicates that PAZ $Cu^{II}$ and PAZ $Zn^{II}$ bind with equal affinity to NiR and both in a fast-exchange mode. The strong linebroadening, which is already observed in the presence of small amounts of NiR, is evidence of an affinity that is higher than in the weak fast-binding mode of the PAZ $Cu^{I}$.

The $\Delta\delta_{Avg}$ values at a molar ratio of 0.15 of either the reduced form of NiR ($Cu^{I}$-T2D) or the oxidised form ($Cu^{II}$–$Cu^{II}$) over PAZ $Zn^{II}$ are plotted for all PAZ residues in Figure 2b and c, respectively, and mapped onto a surface representation of PAZ in Figure 3b and c.

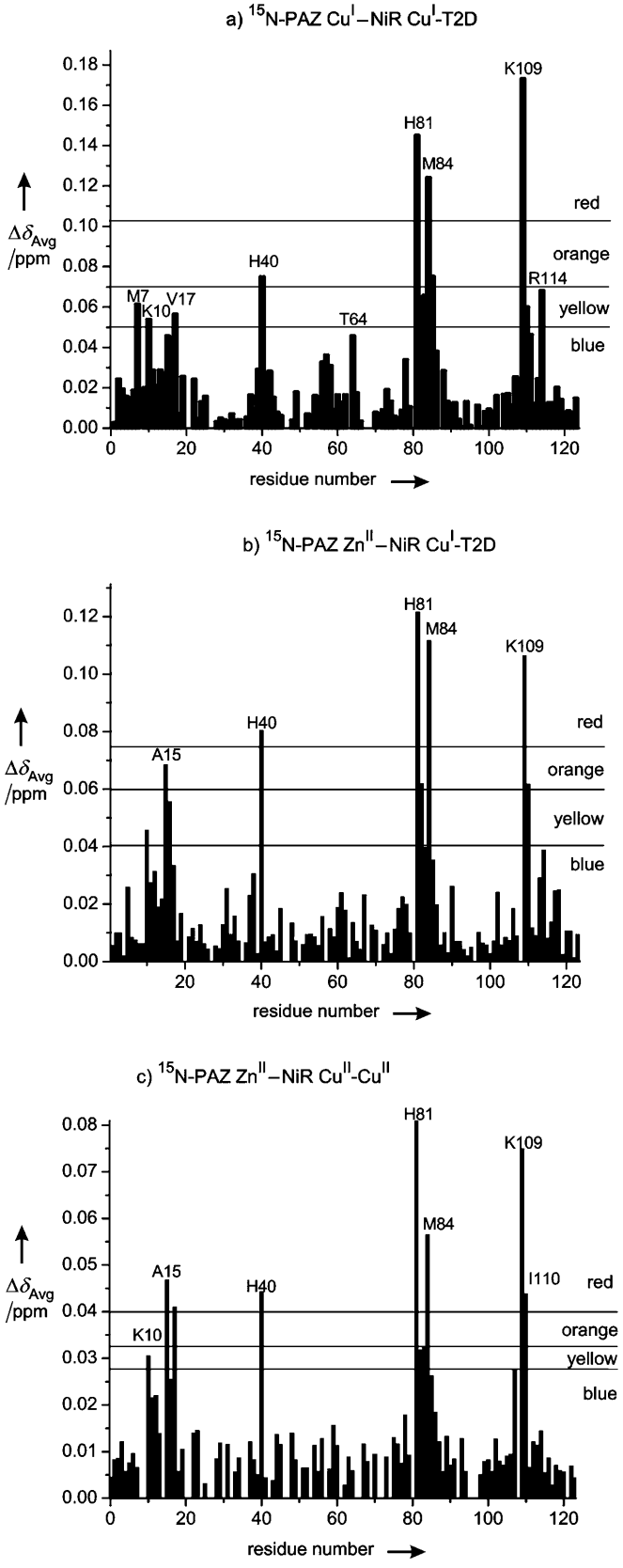


**Figure 2.** Average chemical-shift perturbations ($\Delta\delta_{Avg}$) upon complex formation between a) NiR $Cu^{I}$-T2D and $^{15}N$-PAZ $Cu^{I}$ at a ratio of 1.7, b) NiR $Cu^{I}$-T2D and $^{15}N$-PAZ $Zn^{II}$ at a ratio of 0.15 and c) NiR $Cu^{II}$–$Cu^{II}$ and $^{15}N$-PAZ $Zn^{II}$ at a ratio of 0.10. The horizontal lines indicate the colour code given to the protein surface in the corresponding panel of Figure 3.

  

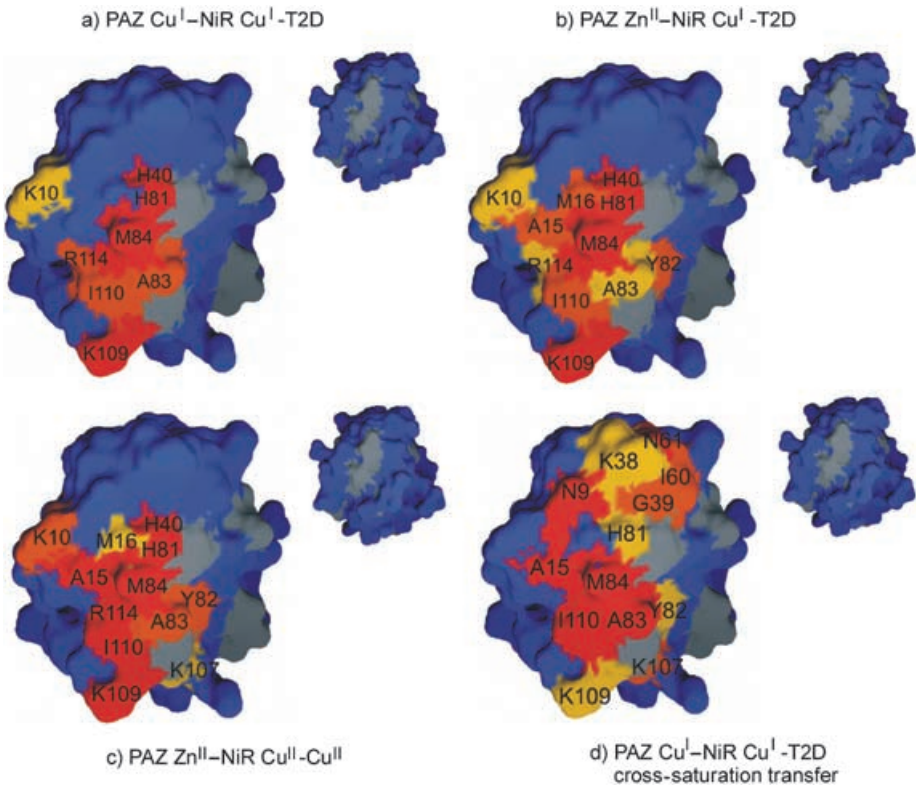


**Figure 3.** Mapping of the $\Delta\delta_{Avg}$ on the surface of PAZ (front side on the left and back side on the right) for the complexes a) NiR Cu$^{I}$-T2D–$^{15}$N-PAZ Cu$^{I}$ at a ratio of 1.7, b) NiR Cu$^{I}$-T2D–$^{15}$N-PAZ Zn$^{II}$ at a ratio 0.15, c) NiR Cu$^{II}$–Cu$^{II}$–$^{15}$N-PAZ Zn$^{II}$ at a ratio of 0.10, d) map obtained with cross-saturation transfer for complex formation between NiR Cu$^{I}$-T2D and $^{15}$N-PAZ Cu$^{I}$ at a ratio of 0.7.[9] Residues in (a)–(c) are colour-coded according to perturbation sizes, with the levels shown in Figure 2. Grey areas indicate Pro or unassigned residues.

It can be concluded that the same patch on the PAZ surface is involved in complex formation between PAZ Zn$^{II}$ and NiR Cu$^{I}$-T2D or NiR Cu$^{II}$–Cu$^{II}$. Furthermore, the similarity between the binding maps for PAZ Cu$^{I}$ and PAZ Zn$^{II}$ is striking, given the difference in the binding modes for both redox states.

### Docking calculations

Docking calculations were carried out with the programme BiGGER.[11,12] Experimental results derived from NMR chemical-shift perturbations were used as constraints. A new algorithm was applied, which restricts the docking search from the start so that all models generated fit the constraints. The calculations yield an ensemble of 5000 model structures for the complex, selected on the basis of best surface matching and ranked according to computational score functions.

The results obtained are presented in Figure 4. The top 200 docking solutions suggest a single PAZ-binding site on each NiR subunit (Figure 4a) with a distance of ~14 Å between the copper ions in PAZ and the type 1 site in NiR (Figure 4b). The distance between the two exposed histidine copper ligands in PAZ and NiR type 1 copper sites is ~8 Å. Figure 4c shows the NiR residues that are within 4 Å of PAZ in at least 30% of the top 200 docking solutions, and they thus comprise the putative binding site for PAZ. Many of the residues are nonpolar, with a ridge of negatively charged residues formed on the side by Glu197, Asp201, Glu204 and Asp205. For PAZ, residues Lys10, Lys38, Lys46, Lys57, Lys77, Lys106 and Lys109 form a

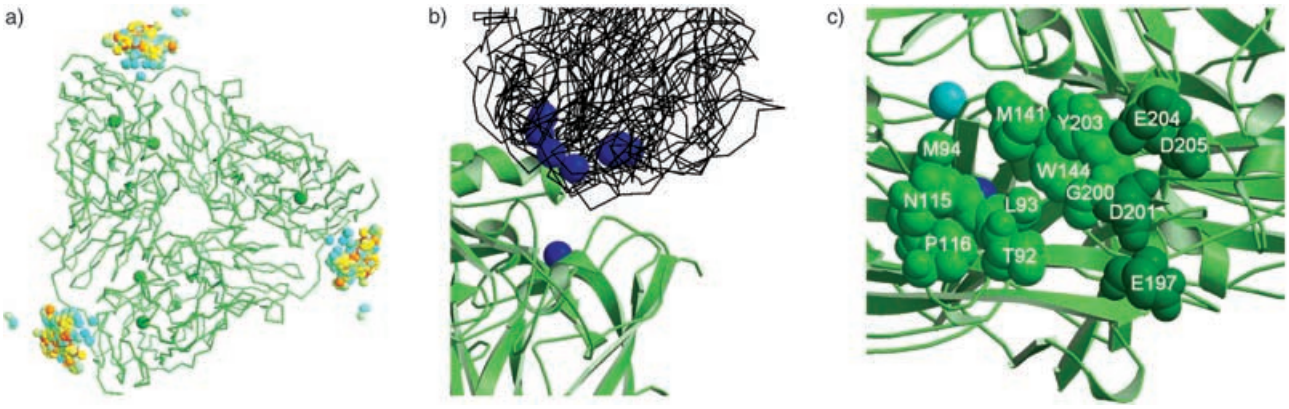


**Figure 4.** Docking of NiR and PAZ. a) The geometrical centre of PAZ of the top 200 orientations obtained in the docking simulations are shown as spheres in relation to NiR (C$^{\alpha}$ trace and copper ions as spheres in green). The PAZ centres are coloured according to their ranking, with red and blue representing the highest and lowest rank. A symmetry operation was conducted to show the same PAZ distribution at each NiR subunit. b) Top seven orientations of PAZ (C$^{\alpha}$ traces) and NiR (green ribbons) are shown to indicate the distance between the type 1 copper ions (blue spheres) in PAZ and NiR. c) The residues that are part of the NiR-binding site predicted from the docking simulations are shown in space-filling representation, with acidic residues in dark green. The remainder of NiR is shown in ribbons. The type 1 and type 2 copper ions are shown as blue and cyan spheres, respectively.

  

ring of positive charges that lines the interface and is close to the surface of NiR. Among these, residues 10, 38, 57 and 77 were shown to be important for the binding affinity in a mutagenesis study.[7]

The model presented here suggests a binding site for PAZ on NiR that is similar to a docking model based on surface complementarity and electrostatics.[13] The orientation of PAZ is rotated between the two models by about 90°. However, in both cases the docking procedures gave an ensemble of PAZ orientations that varied mostly because of rotational freedom. More experimental data will be required to define the structure of the complex better.

## Discussion

The interaction between PAZ and NiR shows a remarkable dependence on the redox state of PAZ, yet a comparison of the binding maps obtained for the fast-exchange mode of both PAZ $Cu^{I}$ and PAZ $Cu^{II}$ indicates that the same surface area is involved in complex formation. In fact, the pattern of the individual $^{15}N$ and $^{1}H$ chemical-shift perturbations observed in the HSQC spectra is also very similar. This suggests that they are a consequence of binding to the same area on NiR, although there is no direct evidence for that.

The binding map obtained through cross-saturation transfer[9] is shown in Figure 3d and exhibits a similar, albeit larger, area that is affected by complex formation. It was argued[9] that the results obtained with this method represent the binding interface in the slow-binding mode. According to this map, similar residues as in the chemical-shift perturbation maps are involved in binding, as well as residues around Ile60. This could indicate a more extensive binding area in the tight slow-binding mode.

It is not clear why PAZ $Cu^{I}$ exhibits two binding modes, while PAZ $Cu^{II}$ shows only fast binding. The most obvious difference between both redox states is the fact that only in the reduced PAZ the copper ligand His81 becomes protonated, with a $pK_a$ of 4.8 (results not shown). This ligand is in the middle of the binding site, so a rearrangement of the imidazole ring after protonation could enhance or decrease the surface matching and thus the affinity. Studies to test whether this protonation is the cause of the redox state-dependent binding are in progress. Kinetic studies might shed more light on the question whether this phenomenon has any relevance for activity and turnover rate of NiR.

It has been proposed that some complexes exist mainly in a single orientation, for example the complexes of cytochrome *f* and plastocyanin from higher plants[14] and the cyanobacterium *Phormidium laminosum*[15] and the complex of yeast cytochrome *c* peroxidase and cytochrome *c*.[16] In those cases, a specific orientation is maintained for a large part of the lifetime of the complex by both electrostatic and hydrophobic interactions. A consequence of this type of interaction is the occurrence of relatively large chemical-shift perturbations upon complex formation in a localised area of the surface, with a maximum $\Delta\delta_{Avg} \approx 0.3$ ppm or higher, in the fully bound state. Other complexes seem to occur in a dynamic ensemble of conformations, like the complex of myoglobin and cytochrome $b_5$.[17] In these complexes, there is not a single specific orientation, but rather numerous conformations exist with similar energies. In these cases the interaction is predominantly electrostatic. Consequently, chemical-shift perturbations are smaller, with a maximum $\Delta\delta_{Avg} \approx 0.02$ ppm in the fully bound state, and the binding area is less localised.

For the PAZ–NiR complex, the $\Delta\delta_{Avg}$ could not be extrapolated to 100% binding because of the lack of a reliable binding constant. However, in the complex between NiR $Cu^{I}$-T2D and PAZ $Zn^{II}$ at a ratio of 0.15, in which only 15% of PAZ can be in the bound state, a $\Delta\delta_{Avg}$ of 0.12 ppm is observed for His81. This would translate into a $\Delta\delta_{Avg}$ of ~0.7 ppm at 100% bound, which represents a large shift. The same is true for the complex between PAZ $Zn^{II}$ and NiR $Cu^{II}$–$Cu^{II}$. Thus, the PAZ–NiR complex appears to classify as a complex with a well-defined orientation. This is supported by the docking simulations, which produce a single binding site for PAZ on NiR. Also in line with this is the nature of the residues involved in binding. Several of these are nonpolar, both on PAZ and the putative binding site on NiR (Figure 4c), indicating that hydrophobic interactions contribute to the binding. Contact between these apolar patches brings the type I copper centres of both proteins within a distance of 14 Å, which is short enough to allow for rapid ET. Interestingly, Trp144 is also part of this interface. The homologous Trp residue in NiR from *A. xylosoxidans* has recently been shown to be important for ET from its redox partner azurin to NiR.[18]

Also charged residues are part of the interface. Of the lysine residues that contribute to the affinity (Lys10, Lys38, Lys57 and Lys77),[7] only the amide group of Lys10 shows a small chemical-shift perturbation. However, many other chemical shift-perturbation studies of redox-protein complexes have demonstrated that the amide groups of uncharged polar and nonpolar residues in the interface show larger perturbations than those of the charged residues, notwithstanding the established contribution of the latter to the affinity of binding. This can be explained by assuming that the chemical shift of the amide groups is most sensitive to the polarity of the environment, which changes upon binding due to restructuring of the water layer in the interface area.[1] The charge interactions play a role in the initial stage of complex formation, by preorienting the partners[19] but might not lead to large changes in surroundings of their backbone amide groups. Figure 4c shows that the docking calculations suggest that most of the negatively charged residues important for binding,[8] Glu197, Asp201, Glu204 and Glu205, are part of the PAZ-binding site on NiR.

In conclusion, the results presented here demonstrate that PAZ binds NiR with an surface area that comprises copper ligand His81; this suggests that this residue is important in the electronic coupling between the two type 1 copper sites and acts as an exit port for ET. PAZ seems to bind in a well-defined fashion, with both electrostatic attraction and hydrophobic interactions contributing to the complex formation.

  

## Experimental Section

**Protein preparation**: All proteins were produced through heterologous expression in *Escherichia coli*. Uniformly $^{15}$N-labelled PAZ was isolated and purified as described.[20] To replace copper with zinc in PAZ, a solution of KCN (200 mM, 0.5 mL) in Tris-HCl (0.5 M, pH 7.0) was added to PAZ $Cu^{II}$ (1 mM, 0.5 mL) in Tris-HCl (0.1 M, pH 7.0). As soon as the solution had bleached, loosing the characteristic blue colour of PAZ $Cu^{II}$, the sample was loaded onto a G25 column equilibrated with Tris-HCl (0.1 M, pH 7.0) containing $ZnCl_2$ (1 mM). The solution of fractions containing PAZ $Zn^{II}$ was changed to water and then to sodium phosphate buffer (20 mM, pH 7.0) by ultrafiltration and purified further to separate possible traces of unfolded protein on a CM column equilibrated with the same buffer. Under a gradient of NaCl (0–250 mM), PAZ eluted at circa 90 mM NaCl.

Into the expression vector for NiR, which was kindly provided by Dr. M. J. Boulanger and Prof. M. E. P. Murphy (UBC, Vancouver, Canada), a stop codon was introduced immediately 3′ of the sequence coding for the native protein, to obtain NiR without a His tag. A 10 mL 2xYT preculture containing kanamycin (100 mg $L^{-1}$), which was incubated at 30 °C and 250 rpm for 6 h, was used to inoculate 1 L of the same medium, which was incubated until $OD_{600} = 1.0$. Expression was induced by addition of isopropylthio-β-D-galactoside (IPTG; 0.5 mM). At this point, the temperature was lowered to 25 °C and after 10 h the cultures were harvested through centrifugation. Cell pellets were resuspended in phosphate buffer (20 mM, pH 7.0) containing NaCl (500 mM), phenylmethylsulfonylfluoride (1 mM), DNAse and $CuCl_2$ (0.5 mM) and lysed by using a French press cell (15.000 PSIG). After centrifugation (15 min, 10.000 rpm) the supernatant was dialysed against phosphate buffer (20 mM, pH 7.0) and loaded onto a DEAE column. With a gradient of NaCl (0–250 mM), NiR eluted at about 140 mM. Fractions containing NiR were concentrated and purified further on a Superdex 75 FPLC gel filtration column. The absorbance ratio $A_{280\,nm}/A_{468\,nm}$ of NiR was 16, and the yield was 150 mg $L^{-1}$. NiR Cu-T2D was obtained following the published procedure.[21] Copper depletion was checked by electron paramagnetic resonance.

Protein concentrations were determined optically by following the characteristic absorbance peaks at 593 nm for PAZ $Cu^{II}$ ($\varepsilon = 2.9\ mM^{-1}cm^{-1}$)[22] and at 277 nm for PAZ $Zn^{II}$ ($\varepsilon = 5.7\ mM^{-1}cm^{-1}$), assuming that at that wavelength PAZ $Cu^{II}$ and PAZ $Zn^{II}$ have the same extinction coefficient. For NiR $Cu^{II}$–$Cu^{II}$ the concentration was determined optically by measuring the absorbance at 589 nm ($\varepsilon = 2.9\ mM^{-1}cm^{-1}$ per subunit).[4]

**NMR experiments and samples**: Two different NMR experiments were performed: direct titration and inverse titration. In the direct titration, a sample containing $^{15}$N-PAZ (0.2 mM) was titrated with microliter aliquots of unlabelled NiR (1.3 mM trimer concentration). In the inverse titration, a sample containing unlabelled NiR (0.4 mM, subunit concentration) was titrated with microliter aliquots of $^{15}$N-PAZ (3.9 mM). Both experiments were performed by recording $^{1}$H,$^{15}$N-HSQC spectra after each addition and analysing the changes in intensity, line width and chemical shift of $^{15}$N-PAZ resonances. For each titration experiment a reference spectrum of the free protein ($^{15}$N-PAZ $Cu^{I}$ or $^{15}$N-PAZ $Zn^{II}$) was recorded. All samples contained phosphate (20 mM, pH 6.5). Samples in the reduced form contained sodium ascorbate (1.0 mM) and were prepared in an anaerobic vial. All NMR samples contained $D_2O$ (6–10% *v/v*) for lock and the solutions were degassed by blowing argon over the surface. For each titration, samples of PAZ and NiR were set at the same pH and the pH was checked at the end of the titration.

**NMR spectroscopy and data analysis**: All NMR experiments were performed at 14.1 T on a Bruker DMX600 spectrometer operating at 293 K and equipped with a TXI-Z-GRAD ($^{1}$H, $^{13}$C and $^{15}$N) probe. All spectra were processed in AZARA (http://www.bio.cam.ac.uk/azara/) and analysed with the assignment programme ANSIG for Windows.[23,24] Assignments for $^{15}$N-PAZ $Cu^{I}$[20] and $^{15}$N-PAZ $Zn^{II}$[10] were taken from the literature.

The average chemical-shift perturbation ($\Delta\delta_{Avg}$) was calculated by using the equation[25] $\Delta\delta_{Avg} = (\Delta\delta_N^2/25 + \Delta\delta_H^2)^{0.5}$, in which $\Delta\delta_N$ and $\Delta\delta_H$ represent the change in the chemical shifts of the amide nitrogen atom and proton, respectively.

**Docking simulations**: The programme BiGGER[11,12] (http://www.dq.fct.unl.pt/bioin/chemera) was used for docking of PAZ and NiR with the PDB entries 8PAZ and 1AQ8 as input files, respectively. The following residues on the PAZ surface were used as constraints for the docking calculation because they show the largest chemical-shift perturbations: Lys10, Ala15, Met16, Val17, His40, His81, Tyr82, Ala83, Met84, Lys107, Lys109, Ile110 and Arg114. The constraint imposed was that at least eight of these 13 residues on the PAZ surface are in contact with NiR. Remarkably, inspection of the 200 highest-ranking complexes provides very similar results either with or without experimental constraints. Considering more than 200 ranking solutions does not change the results.

Results were obtained for docking at just one side of the NiR trimer and thus a symmetry operation was performed to generate the distributions for the three subunits shown in Figure 4a.

## *Acknowledgements*

*The Netherlands Organisation for Scientific Research (NWO, Grant 700.99.512) and the Fundação para a Ciencia e Tecnologia (Grant BPD 12328/03) are acknowledged for financial support.*

**Keywords:** electron transfer · metalloproteins · nitrite reductase · NMR spectroscopy · pseudoazurin

[1] P. B. Crowley, M. Ubbink, *Acc. Chem. Res.* **2003**, *36*, 723–730.
[2] M. Prudêncio, M. Ubbink, *J. Mol. Recognit.* **2004**, *17*, 524–539.
[3] E. T. Adman, *Adv. Protein Chem.* **1991**, *42*, 145–197.
[4] T. Kakutani, H. Watanabe, K. Arima, T. Beppu, *J. Biochem.* **1981**, *89*, 453–461.
[5] K. Petratos, D. Dauter, K. S. Wilson, *Acta Crystallogr. Sect. B Struct. Sci.* **1988**, *44*, 628–636.
[6] M. E. Murphy, S. Turley, E. T. Adman, *J. Biol. Chem.* **1997**, *272*, 28455–28460.
[7] M. Kukimoto, M. Nishiyama, T. Ohnuki, S. Turley, E. T. Adman, S. Horinouchi, T. Beppu, *Protein Eng.* **1995**, *8*, 153–158.
[8] M. Kukimoto, M. Nishiyama, M. Tanokura, E. T. Adman, S. Horinouchi, *J. Biol. Chem.* **1996**, *271*, 13680–13683.
[9] A. Impagliazzo, M. Ubbink, *J. Am. Chem. Soc.* **2004**, *126*, 5658–5659.
[10] M. Prudêncio, J. Rohovec, J. A. Peters, E. I. Tocheva, M. J. Boulanger, M. E. P. Murphy, H. J. Hupkes, W. Kosters, A. Impagliazzo, M. Ubbink, *Chem. Eur. J.* **2004**, *10*, 3252–3260.
[11] X. J. Morelli, P. N. Palma, F. Guerlesquin, A. C. Rigby, *Protein Sci.* **2001**, *10*, 2131–2137.
[12] P. N. Palma, L. Krippahl, J. E. Wampler, J. J. Moura, *Proteins* **2000**, *39*, 372–384.
[13] L. M. Murphy, F. E. Dodd, F. K. Yousafzai, R. R. Eady, S. S. Hasnain, *J. Mol. Biol.* **2002**, *315*, 859–871.

  

[14] M. Ubbink, M. Ejdebäck, B. G. Karlsson, D. S. Bendall, *Structure* **1998**, *6*, 323 – 335.
[15] P. B. Crowley, G. Otting, B. G. Schlarb-Ridley, G. W. Canters, M. Ubbink, *J. Am. Chem. Soc.* **2001**, *123*, 10444 – 10453.
[16] J. A. R. Worrall, U. Kolczak, G. W. Canters, M. Ubbink, *Biochemistry* **2001**, *40*, 7069 – 7076.
[17] J. A. R. Worrall, Y. J. Liu, P. B. Crowley, J. M. Nocek, B. M. Hoffman, M. Ubbink, *Biochemistry* **2002**, *41*, 11721 – 11730.
[18] M. L. Barrett, R. L. Harris, S. Antonyuk, M. A. Hough, M. J. Ellis, G. Sawers, R. R. Eady, S. S. Hasnain, *Biochemistry* **2004**, *43*, 16311 – 16319.
[19] J. B. Matthew, P. C. Weber, F. R. Salemme, F. M. Richards, *Nature* **1983**, *301*, 169 – 171.
[20] A. Impagliazzo, M. Ubbink, *J. Biomol. NMR* **2004**, *29*, 541 – 542.
[21] S. Suzuki, Deligeer, K. Yamaguchi, K. Kataoka, K. Kobayashi, S. Tagawa, T. Kohzuma, S. Shidara, H. Iwasaki, *J. Biol. Inorg. Chem.* **1997**, *2*, 265 – 274.
[22] T. Kakutani, H. Watanabe, K. Arima, T. Beppu, *J. Biochem.* **1981**, *89*, 463 – 472.
[23] P. J. Kraulis, *J. Magn. Reson.* **1989**, *84*, 627 – 633.
[24] M. Helgstrand, P. Kraulis, P. Allard, T. Hard, *J. Biomol. NMR* **2000**, *18*, 329 – 336.
[25] D. S. Garrett, Y.-J. Seok, A. Peterkofsky, G. M. Clore, A. M. Gronenborn, *Biochemistry* **1997**, *36*, 4393 – 4398.

Received: February 25, 2005

  